

NeuroMET

Virtual MR Spectroscopy Workshop

L3: Calibration & Workflow

Ariane Fillmer, PhD

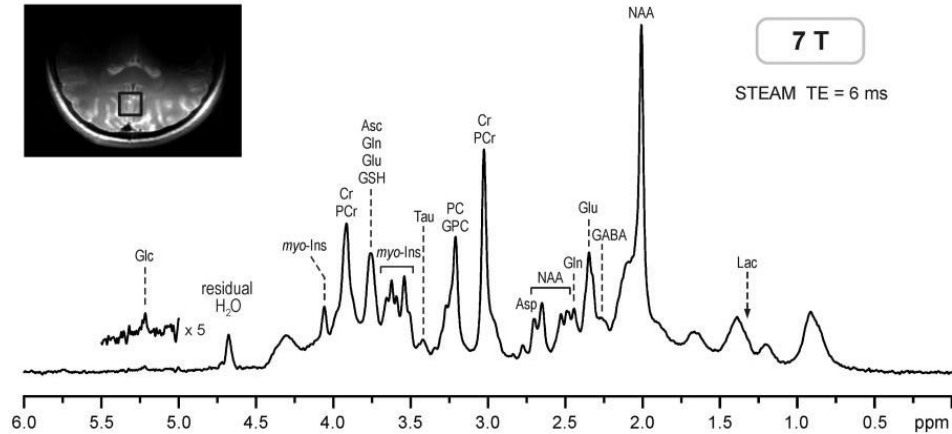
Physikalisch-Technische Bundesanstalt, AG «In-vivo MRT»



NeuroMET



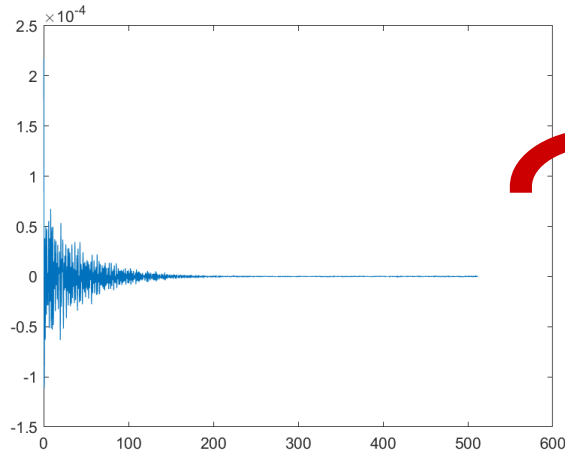
How to ensure high quality in MRS data?



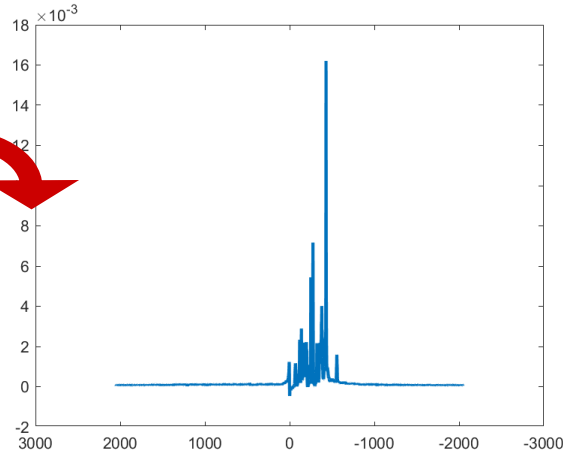
**What constitutes high quality
in MRS data?**

- **Separated peaks:** Spectral resolution, homogeneous B_0 field
- **Well-defined peaks:** Adequate SNR
- **Artifact free Signal**

Spectral Resolution



FT



$T_{\text{acq}} = 512 \text{ ms}$
Sampling rate = $1/250 \text{ ms}$
 $N = 2048$
 $BW = 4000$

T_{acq}

Bandwidth

N number of sample points

$\Delta\nu$ spectral resolution

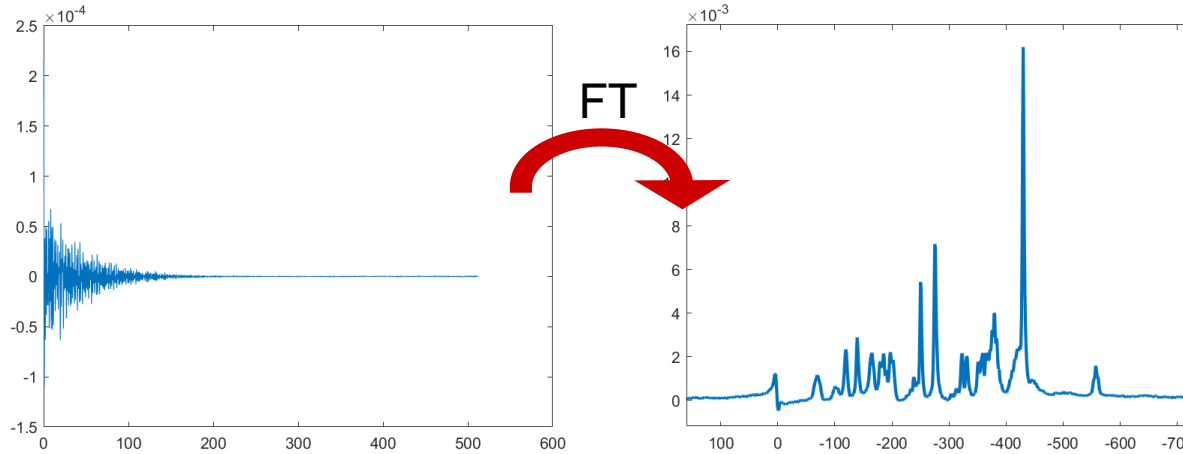
BW spectral bandwidth

$$\Delta\nu = BW / N$$

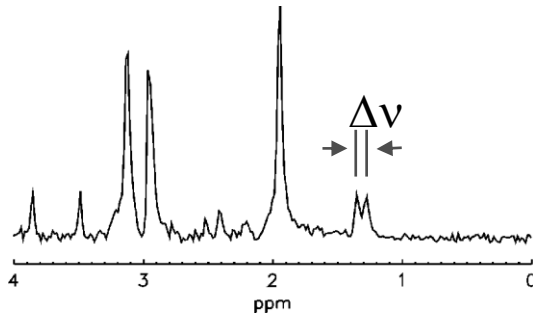
$$\Delta\nu = 1 / T_{\text{acq}}$$

$$T_{\text{acq}} = 1 / \Delta\nu = N / BW$$

Spectral Resolution

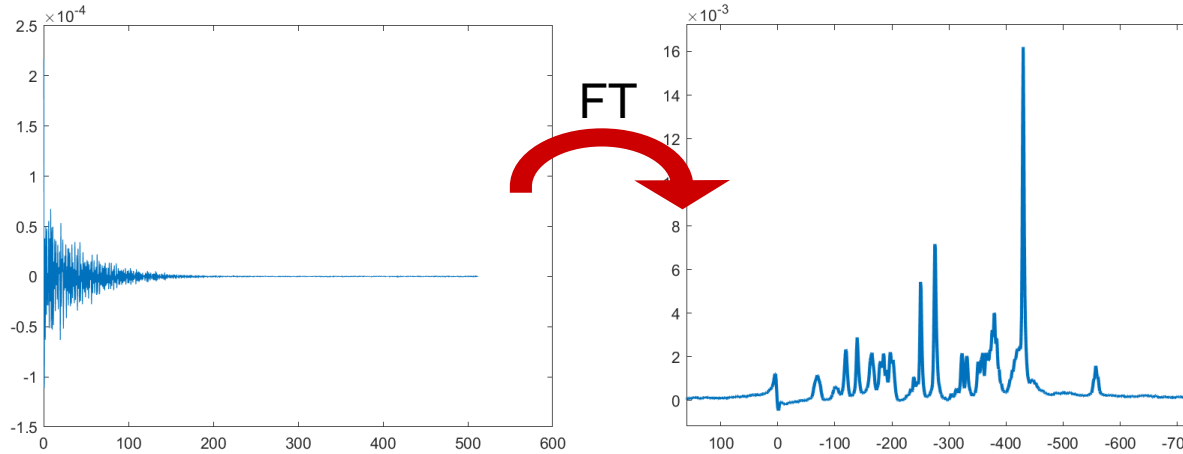


short T_{acq}
→ bad resolution

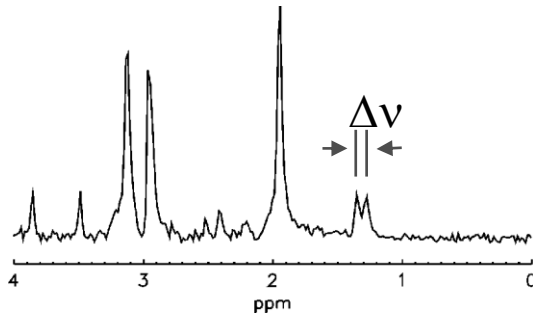


To resolve two peaks with $\Delta\nu = 6$ Hz
→ $\Delta\nu \leq 3$ Hz required, better $\Delta\nu \approx 1$ Hz
 $\Delta\nu = 1 / T_{acq}$
 $T_{acq} = 1 / \Delta\nu$
 $T_{acq} \approx 1$ s

Spectral Resolution

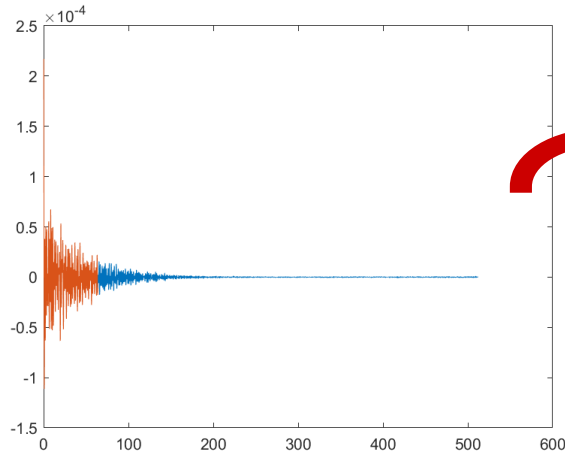


short T_{acq}
→ bad resolution

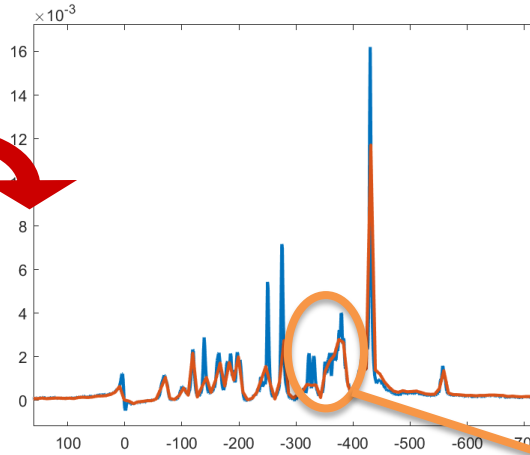


To resolve two peaks with $\Delta\nu = 6$ Hz
→ $\Delta\nu \leq 3$ Hz required, better $\Delta\nu \approx 1$ Hz
 $\Delta\nu = 1 / T_{acq}$
 $T_{acq} = 1 / \Delta\nu$
 $T_{acq} \approx 1$ s

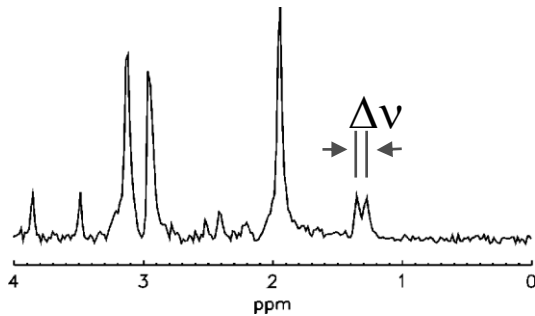
Spectral Resolution



FT



short T_{acq}
→ bad resolution

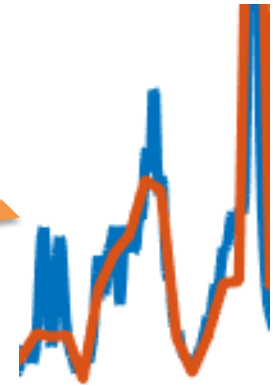


To resolve two peaks with $\Delta\nu = 6$ Hz
→ $\Delta\nu \leq 3$ Hz required, better $\Delta\nu \approx 1$ Hz

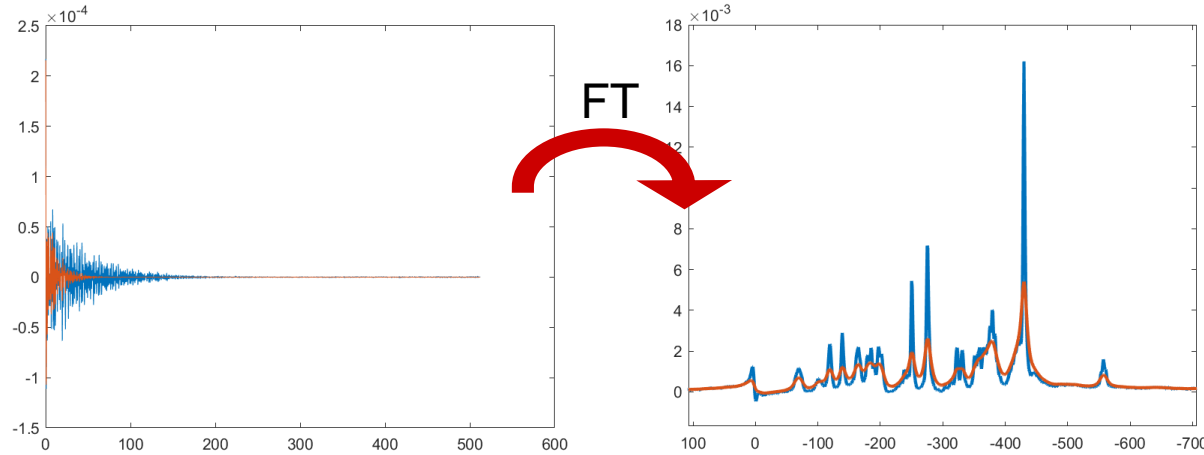
$$\Delta\nu = 1 / T_{acq}$$

$$T_{acq} = 1 / \Delta\nu$$

$$T_{acq} \approx 1 \text{ s}$$

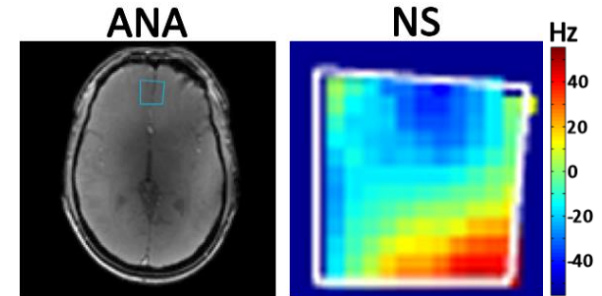


Spectral Resolution

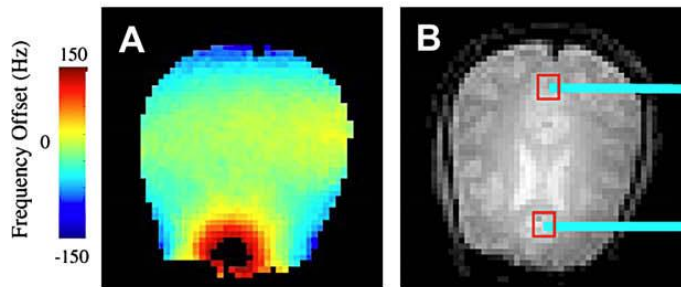


If T_2^* is too short,
resolution decreases
→ broad lines

What causes a short T_2^* ?

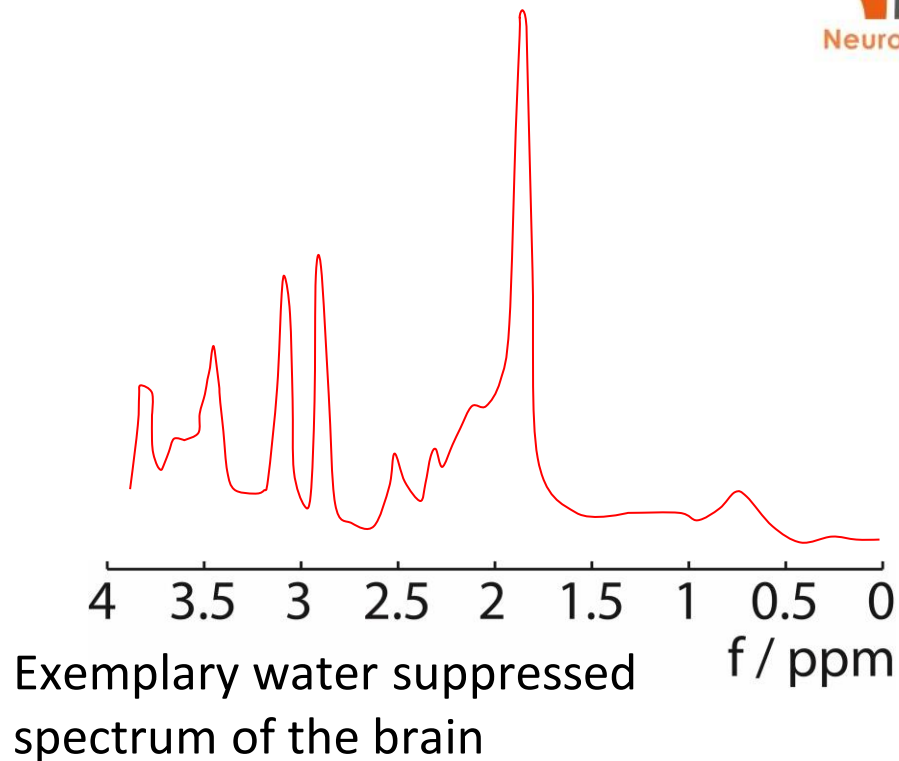


B₀ Shimming



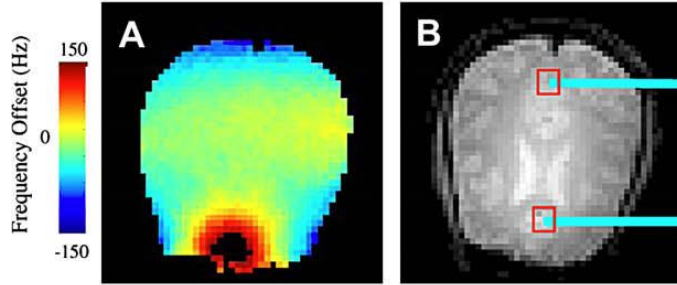
(A) Field map of an axial MRI

(B) Axial MRI with indication of two spectroscopy voxels

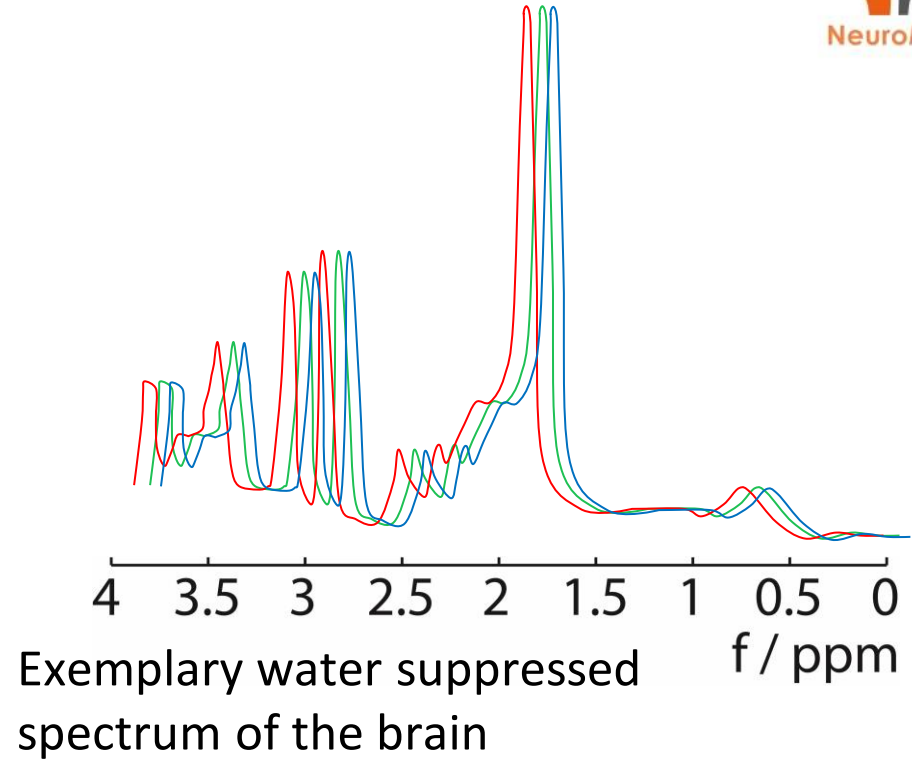


K. Koch et al., Prog. Nuc. Mag. Res. Spec. 54: 69-96 (2009)

B₀ Shimming

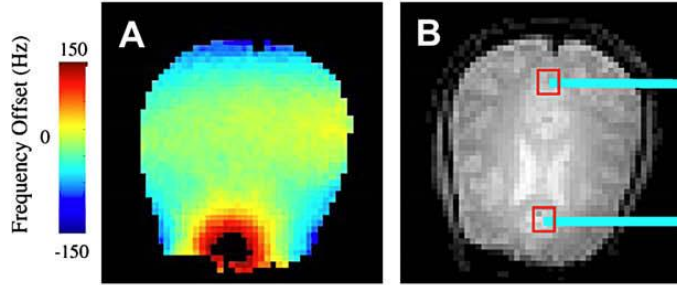


(A) Field map of an axial MRI
(B) Axial MRI with indication of two spectroscopy voxels

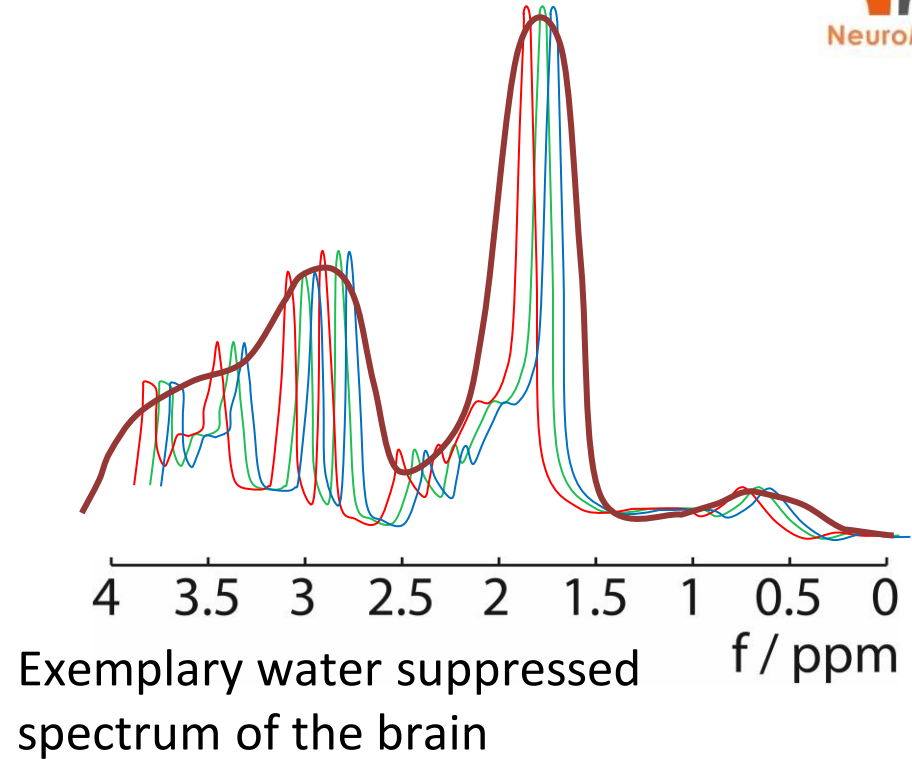


K. Koch et al., Prog. Nuc. Mag. Res. Spec. 54: 69-96 (2009)

B₀ Shimming



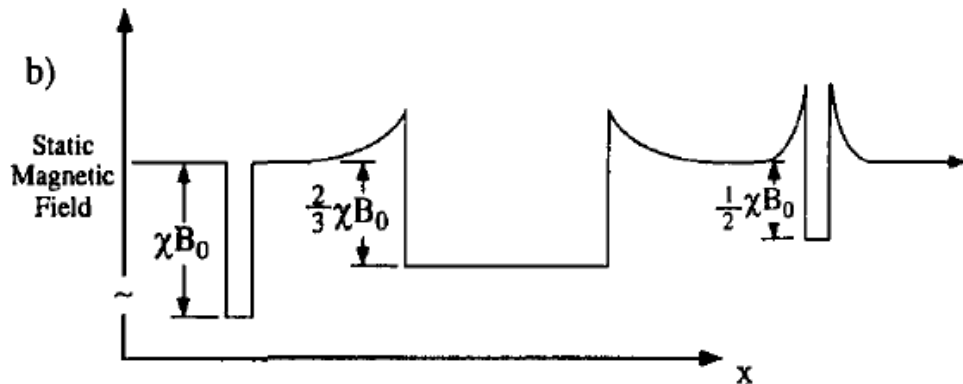
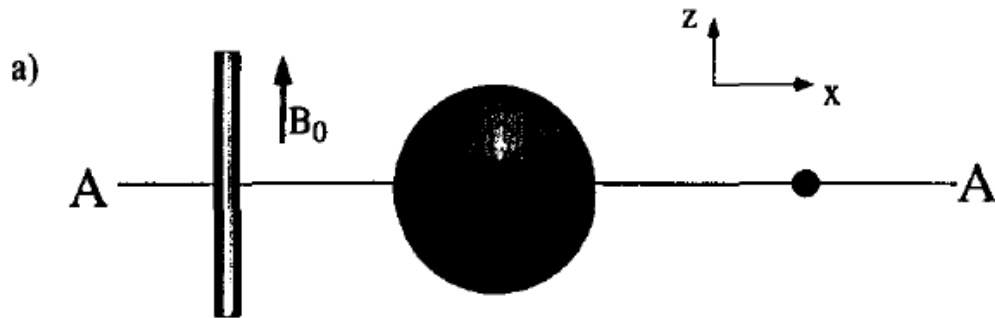
(A) Field map of an axial MRI
(B) Axial MRI with indication of two spectroscopy voxels



K. Koch et al., Prog. Nuc. Mag. Res. Spec. 54: 69-96 (2009)

B_0 Shimming

Effects of Sample Shape, Orientation and Susceptibility
on the Static Magnetic Field



- shape
- orientation
- susceptibility

influence B_0 field
distortion

J.F. Schenck, Med. Phys. 23: 815-850 (1996)

Concepts in Magnetic Resonance, 1990, 2, 131-149

The Ancient and Honourable Art of Shimming

Gwendolyn N. Chmurny* and David I. Hoult

Program Resources, Inc.
National Cancer Institute
Frederick Cancer Research and Development Center
Frederick, Maryland 21701*

Received May 4, 1990

INTRODUCTION

It could be argued with some vehemence that the biggest bane of a high-resolution NMR spectroscopist's existence is the ritual of "magnet shimming." This black art can provoke hyperbole and hypertension, and over the years, based on an inadequate understanding of a complex phenomenon, many myths concerning shimming have arisen. Thus, our aim in this article is two-fold. First, we shall explain the origins of magnetic-field inhomogeneity and the mathematical analysis that leads to the concept of shimming. Second, we shall explore some of the many practical factors that complicate the basic theory and that lead to the complexity that often results in intuition and art, rather than science, controlling the shimming process. We hope, in so doing, to reduce the average blood pressure of NMR spectroscopists!

Field Homogenizing Coils for Nuclear Spin Resonance Instrumentation

MARCEL J. E. GOLAY

The Perkin-Elmer Corporation, Norwalk, Connecticut

(Received September 6, 1957; and in final form, January 27, 1958)

The general arrangement suggested above can be thought of as an extension of the degaussing coils used in ships. The main field is not affected, but the field inhomogeneities are “degaussed” by coils which operate orthogonally to each other.

M. J. E. Golay, Rev. Sci. Inst. 29(4): 313-315 (1958)

USN - U.S. Navy photo 80-GK-5645; U.S. Defense Visual Information Photo HD-SN-99-03026

B₀ Shimming



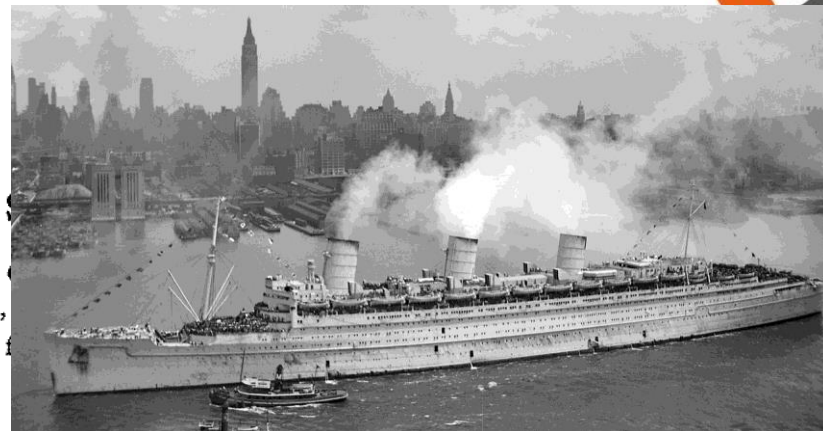
THE REVIEW OF SCIENTIFIC INSTRUMENTS

Field Homogenizing Coils for Nuclear S

MARCEL J. E. G

The Perkin-Elmer Corporation,

(Received September 6, 1957; and in f



The general arrangement suggested above can be thought of as an extension of the degaussing coils used in ships. The main field is not affected, but the field inhomogeneities are “degaussed” by coils which operate orthogonally to each other.

M. J. E. Golay, Rev. Sci. Inst. 29(4): 313-315 (1958)

USN - U.S. Navy photo 80-GK-5645; U.S. Defense Visual Information Photo HD-SN-99-03026

B₀ Shimming



THE REVIEW OF SCIENTIFIC INSTRUMENTS

Field Homogenizing Coils for Nuclear S

MARCEL J. E. G

The Perkin-Elmer Corporation,

(Received September 6, 1957; and in f



The general arrangement suggested above can be thought of as an extension of the degaussing coils used in ships. The main field is not affected, but the field inhomogeneities are “degaussed” by coils which operate orthogonally to each other.

M. J. E. Golay, Rev. Sci. Inst. 29(4): 313-315 (1958)

USN - U.S. Navy photo 80-GK-5645; U.S. Defense Visual Information Photo HD-SN-99-03026

B₀ Shimming



THE REVIEW OF SCIENTIFIC INSTRUMENTS

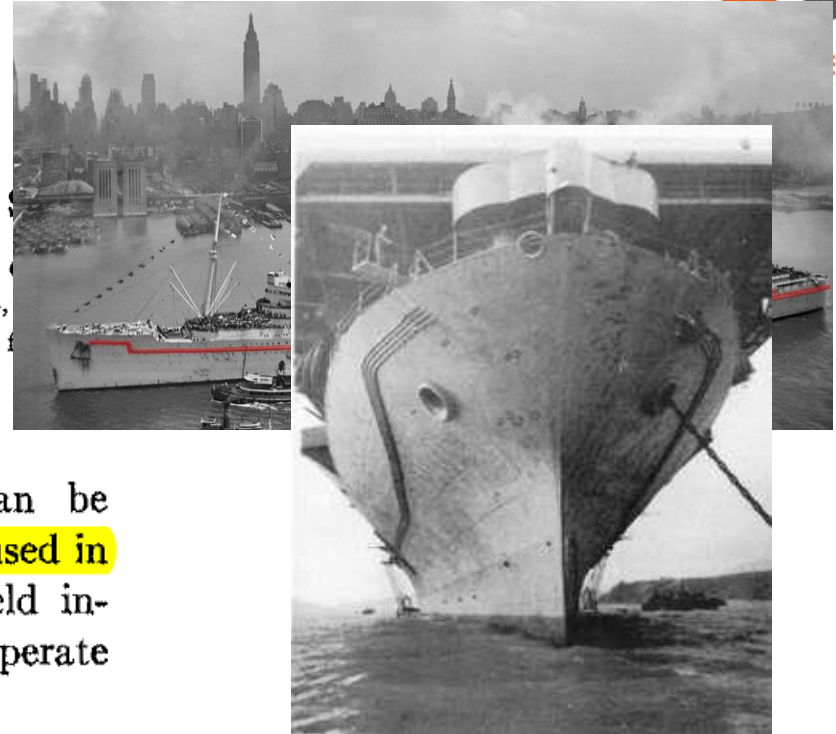
Field Homogenizing Coils for Nuclear S

MARCEL J. E. G

The Perkin-Elmer Corporation,

(Received September 6, 1957; and in f

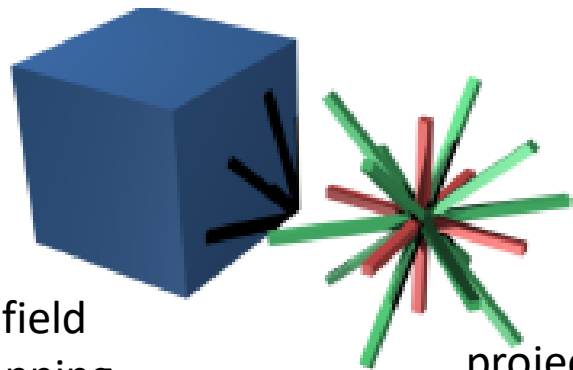
The general arrangement suggested above can be thought of as an extension of the degaussing coils used in ships. The main field is not affected, but the field inhomogeneities are “degaussed” by coils which operate orthogonally to each other.



M. J. E. Golay, Rev. Sci. Inst. 29(4): 313-315 (1958)

USN - U.S. Navy photo 80-GK-5645; U.S. Defense Visual Information Photo HD-SN-99-03026

B₀ Shimming



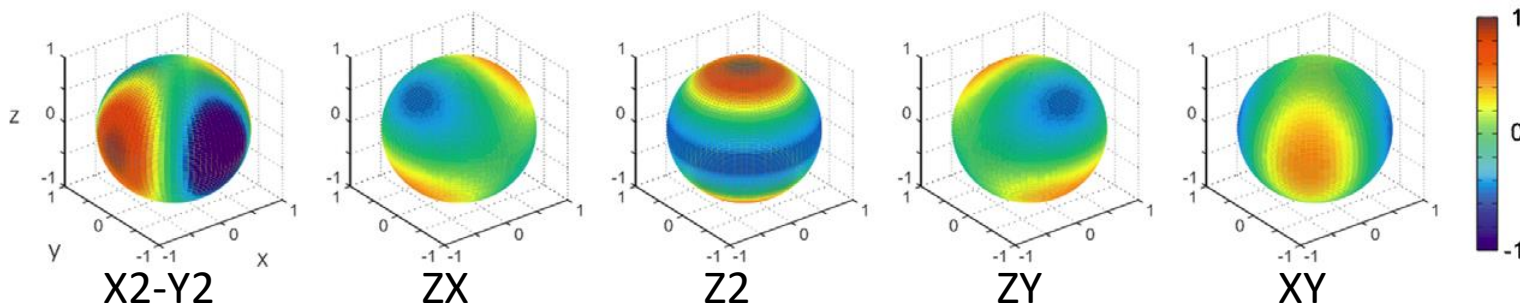
3D field
mapping

projection based
field mapping

Acquisition of Field Map

Decomposition of Field Map into
Basis Functions

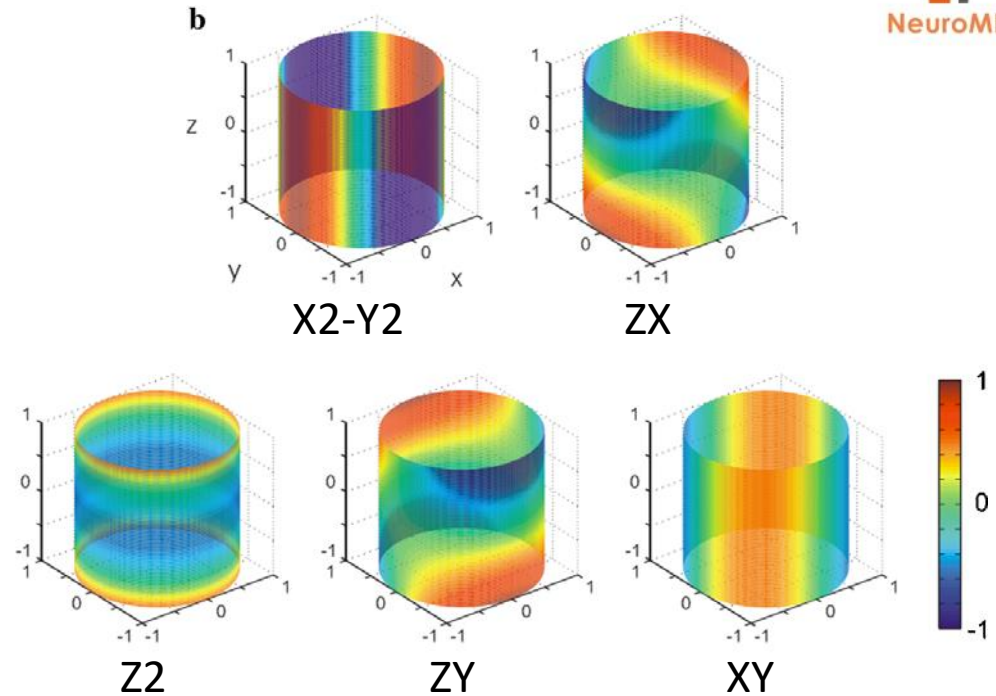
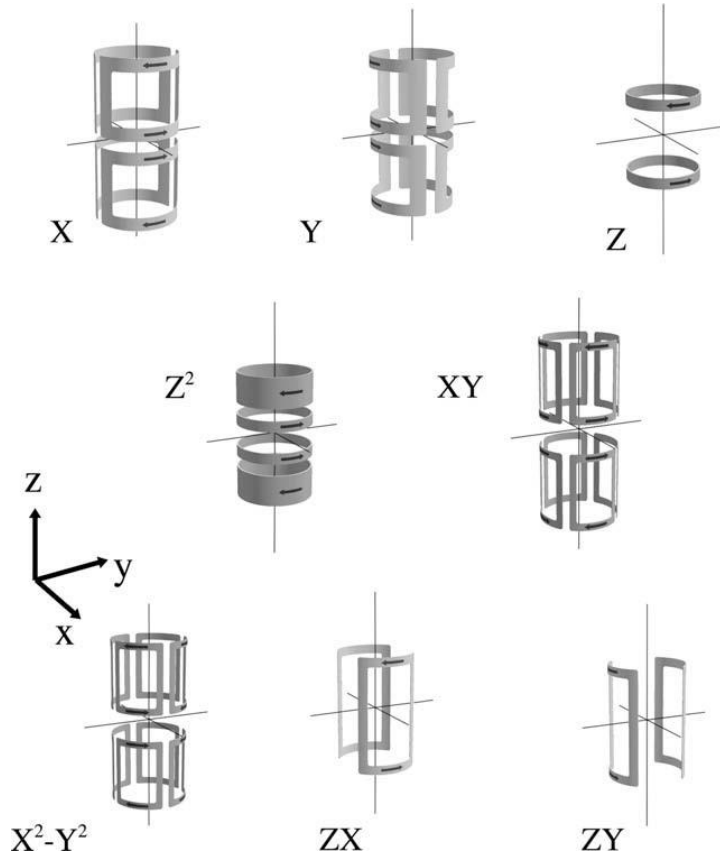
Application of Correction Fields



C. Juchem et al., JMR 183: 278-289 (2006)

M. Poole et al., Benefits of Brain Segmentation and 3D Field Mapping in B₀ Shimming at 7T

B₀ Shimming

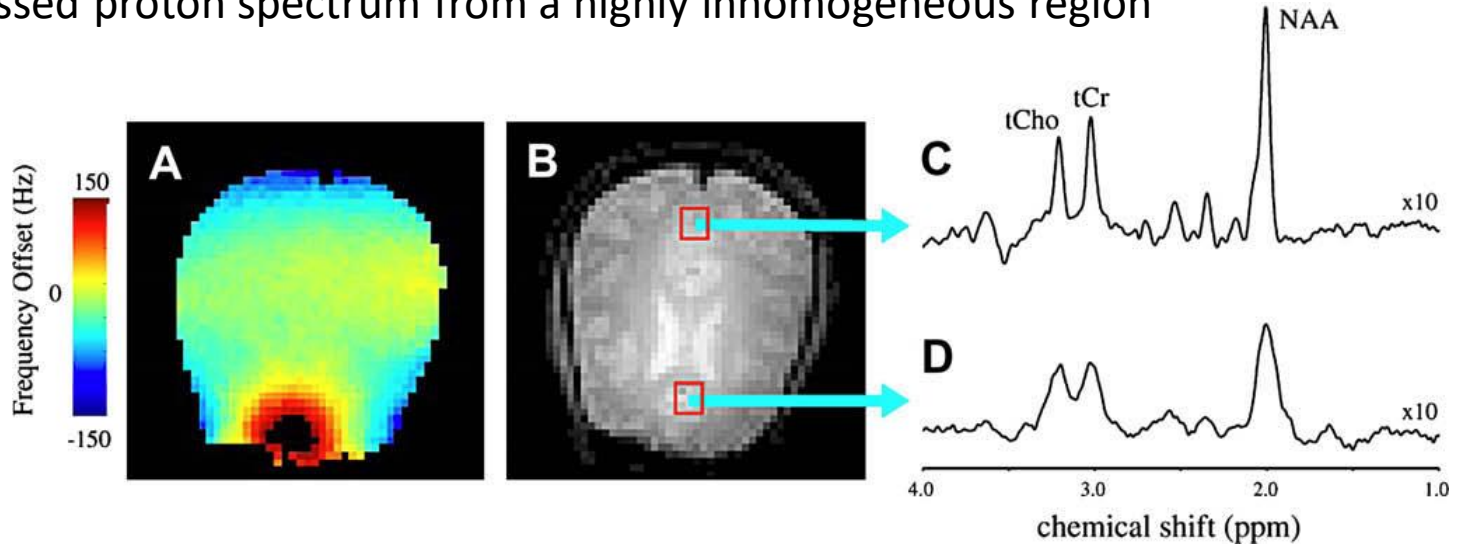


K. Koch et al., Prog. Nuc. Mag. Res. Spec. 54: 69-96 (2009)

C. Juchem et al., JMR 183: 278-289 (2006)

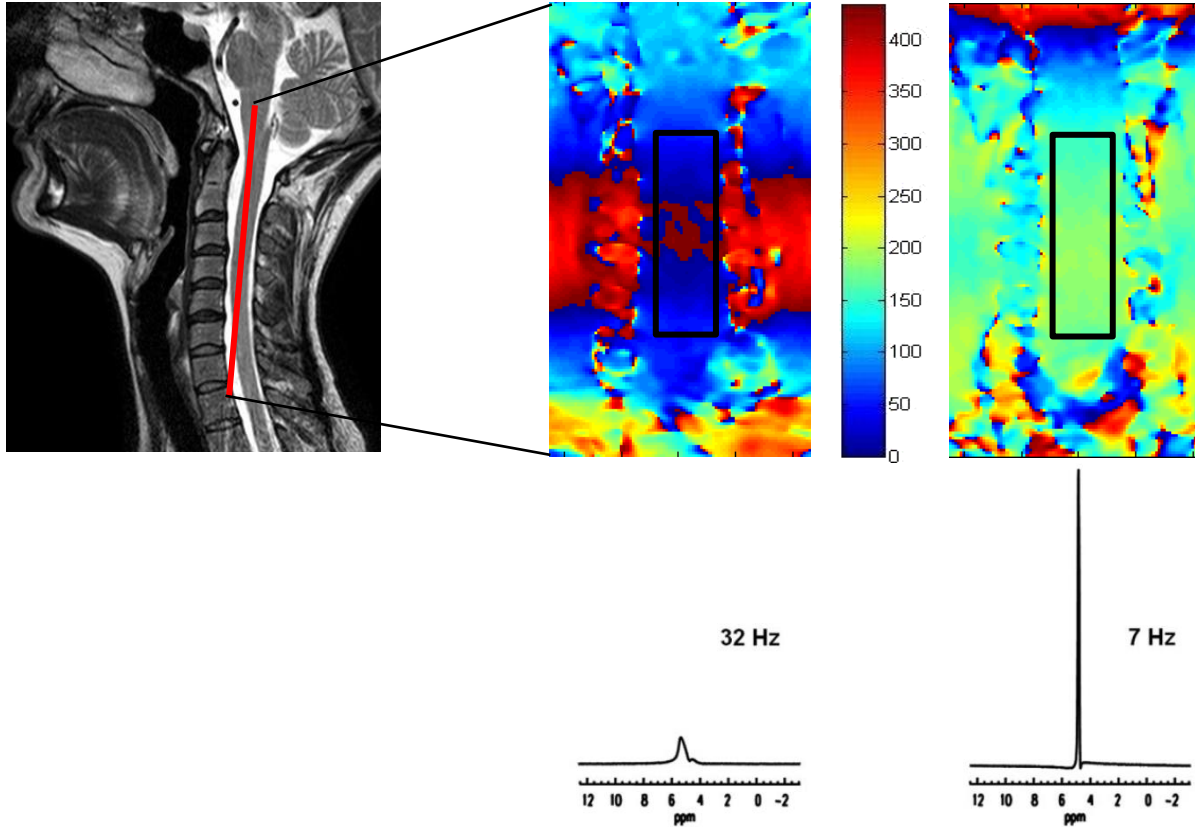
B₀ Shimming

- (A) Field map of an axial MRI
- (B) Axial MRI with indication of two spectroscopy voxels
- (C) Water suppressed proton spectrum from an almost homogeneous region
- (D) Water suppressed proton spectrum from a highly inhomogeneous region



K. Koch et al., Prog. Nuc. Mag. Res. Spec. 54: 69-96 (2009)

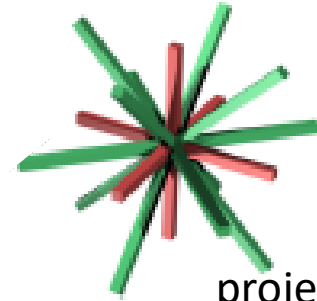
B₀ Shimming



B_0 Shimming

How to B_0 Shim?

- FAST(EST)MAP

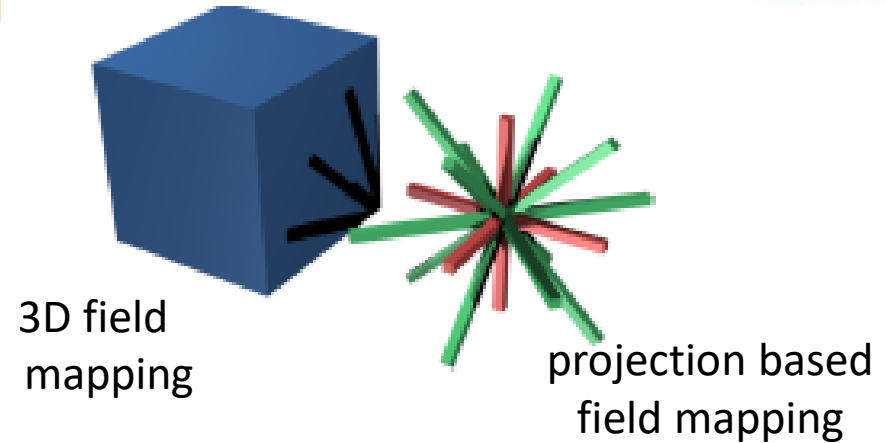


projection based
field mapping

B₀ Shimming

How to B₀ Shim?

- FAST(EST)MAP
- 3D Field Mapping



Questions?

B_0 Shimming

- reduce inhomogeneities
 - ➡ longer $T2^*$
 - ➡ smaller line width and higher amplitudes
- this improves
 - ➡ signal to noise
 - ➡ resolution



Signal-to-Noise Ratio

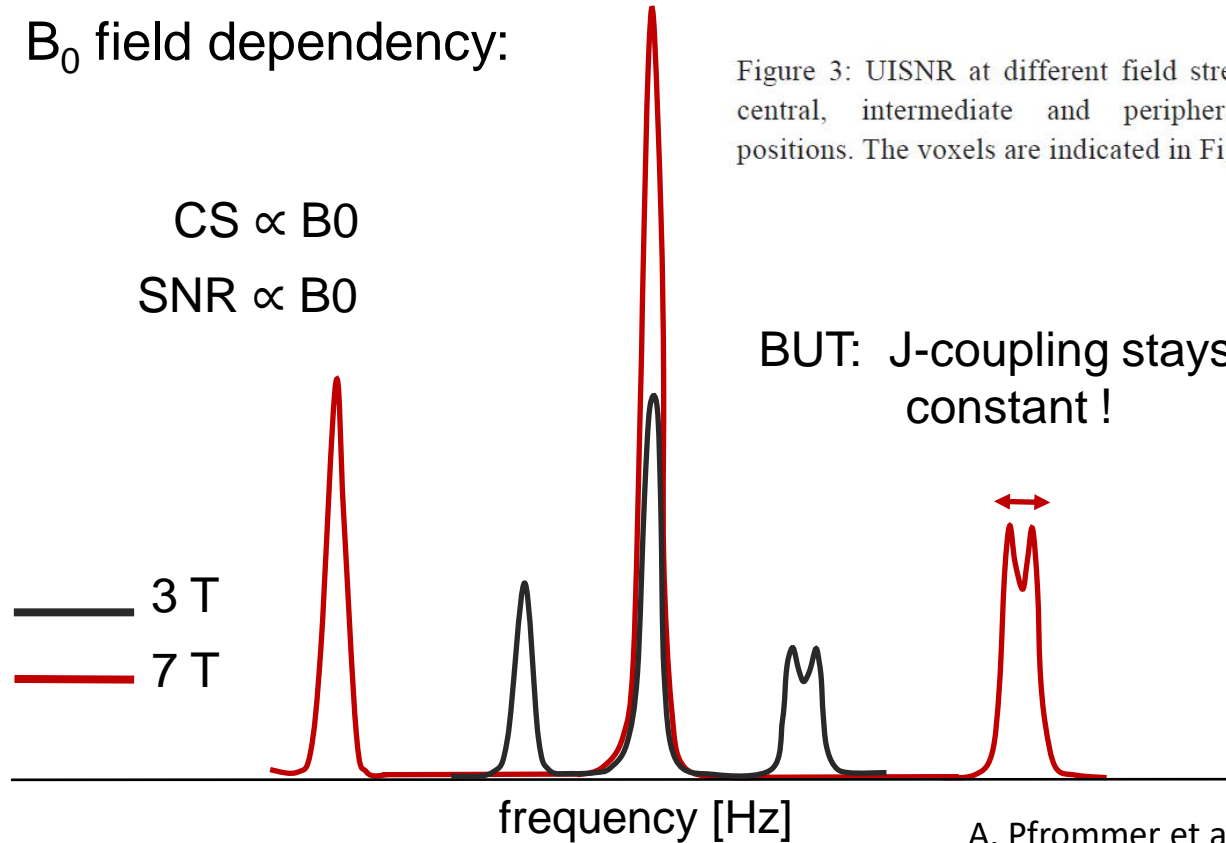


B_0 field dependency:

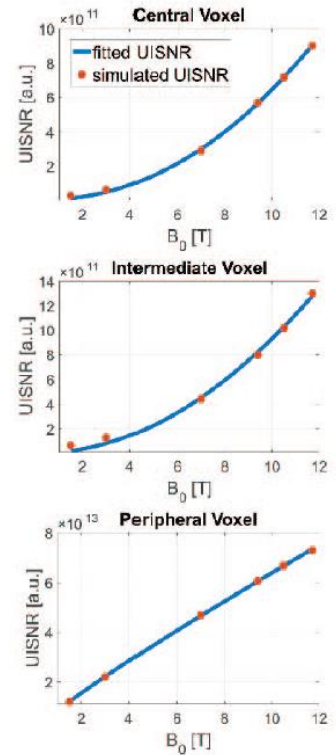
$$CS \propto B_0$$

$$SNR \propto B_0$$

Figure 3: UISNR at different field strengths for central, intermediate and peripheral voxel positions. The voxels are indicated in Figure 4.



BUT: J-coupling stays constant !



A. Pfrommer et al., Doi: [10.1109/ICEAA.2017.8065339](https://doi.org/10.1109/ICEAA.2017.8065339)

Signal-to-Noise Ratio



How to optimize SNR?

B_1 calibration

RF calibration

Power Optimization

Flip Angle Calibration

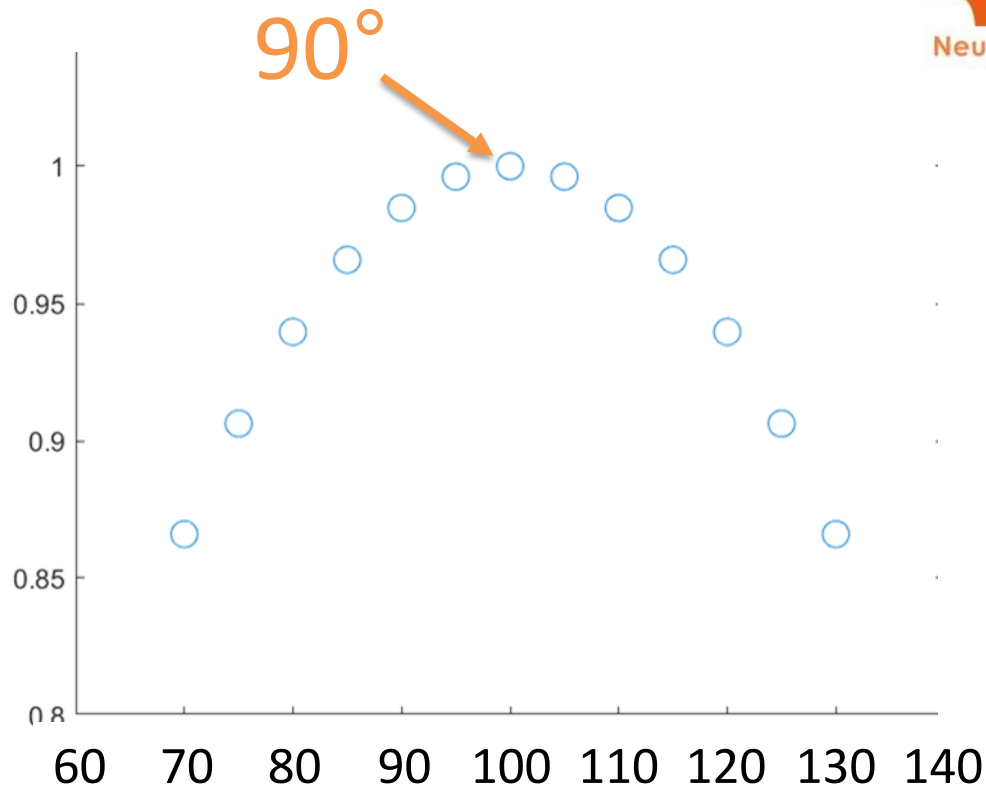
Making sure a 90° flip angle actually flips the magnetization by 90°

$$\alpha = \gamma \cdot B_1 \cdot t_P$$

Signal-to-Noise Ratio



Making sure a 90° flip angle actually flips the magnetization by 90°



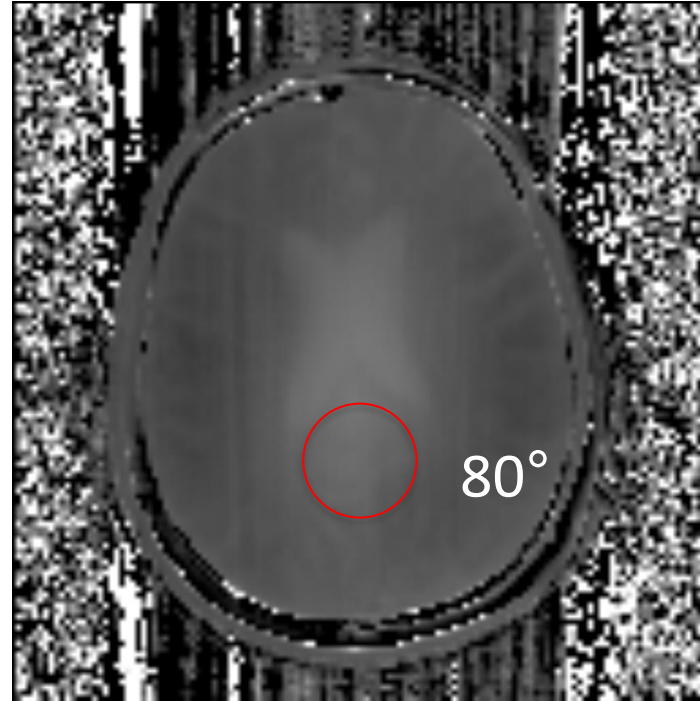
Signal-to-Noise Ratio

Flip Angle Map

B₁ Map

$$\frac{\text{RefVoltage}}{\text{measFA}} \cdot \text{targetFA}$$

$$\frac{200 \text{ V}}{80^\circ} \cdot 90^\circ = 225 \text{ V}$$



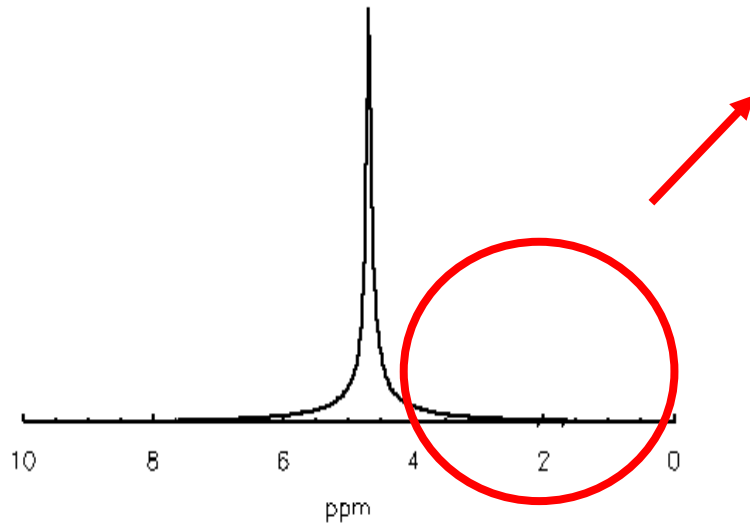
Reference voltage: 200 V

Questions?

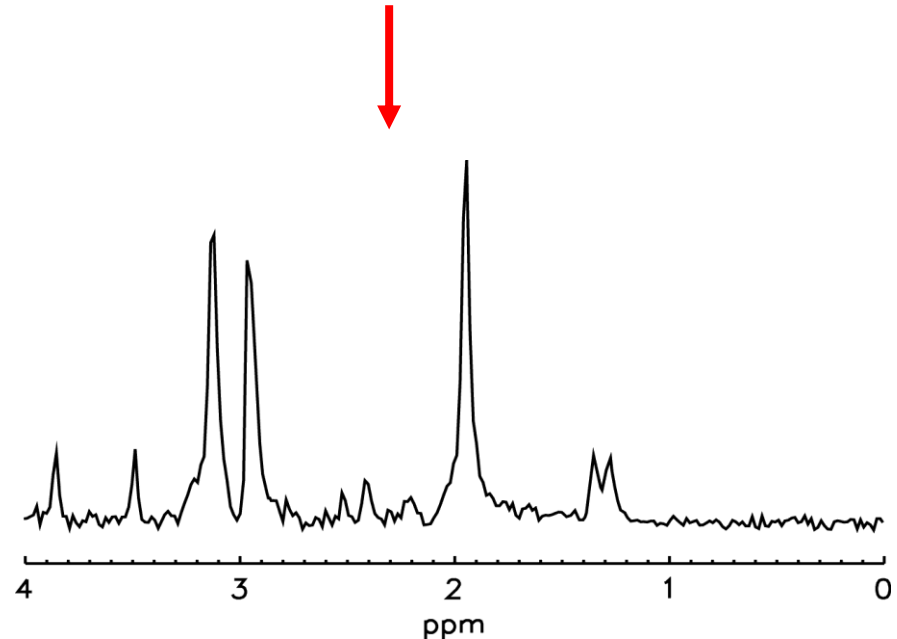


Water Suppression

We are interested in the *small* peaks



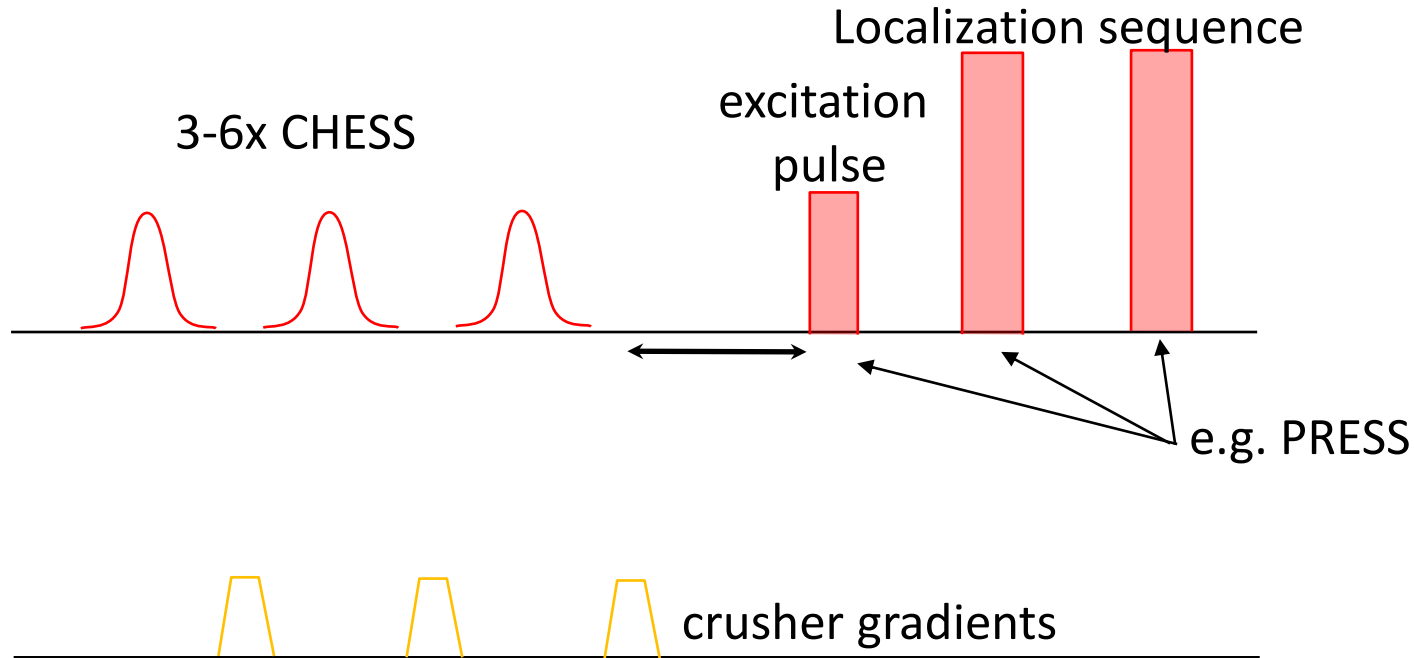
Water suppression



Brain water: 10^2 mol/l
Brain metabolites: $10^{-4} - 10^{-2}$ mol/l
High dynamic range required: $\sim 10^5$

Water Suppression

Chemical Shift Selective excitation



Water Suppression

frequency selective
adiabatic pulse

RF

90°

90° pulse (start of sequence,
e.g. PRESS)

short delay

crusher
gradients

water
magnetization:

$> 90^\circ$

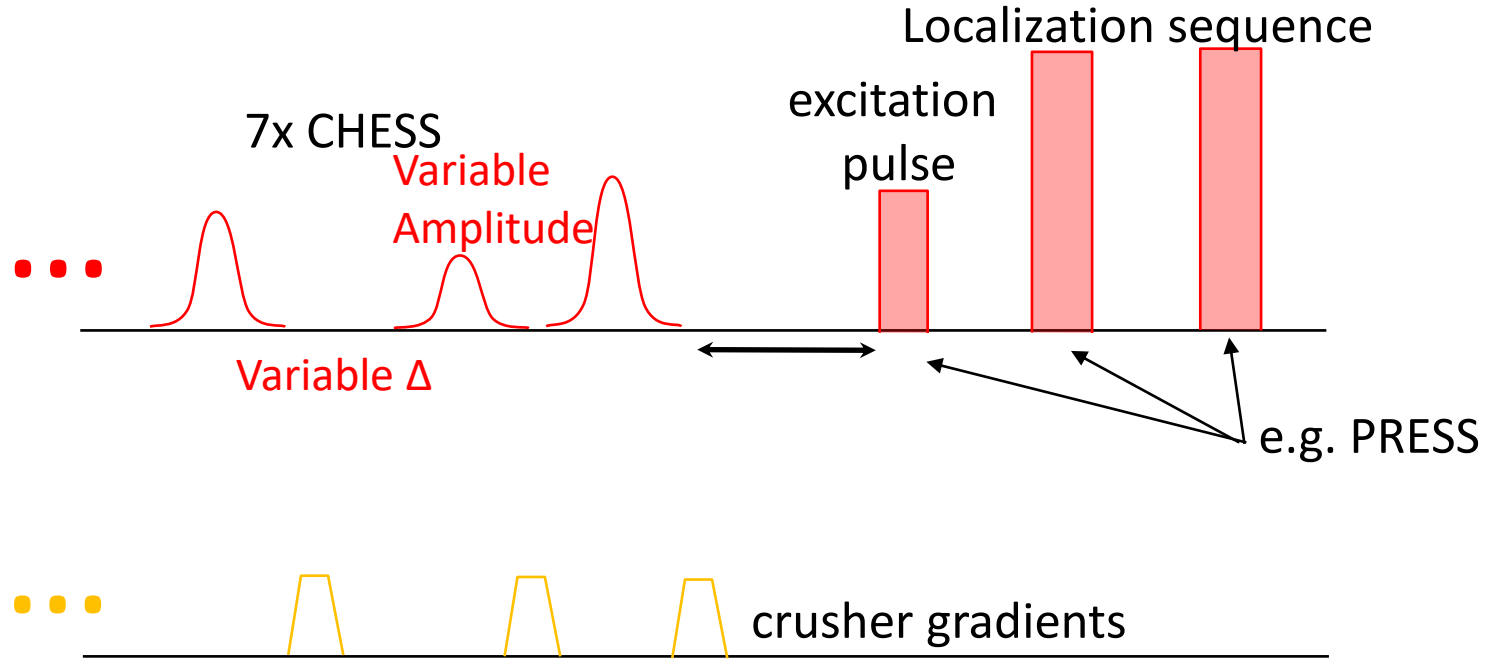
after crusher gradients

after delay

residual water

Water Suppression

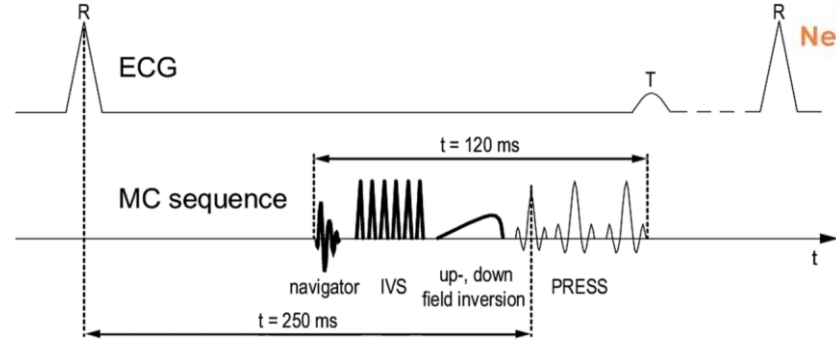
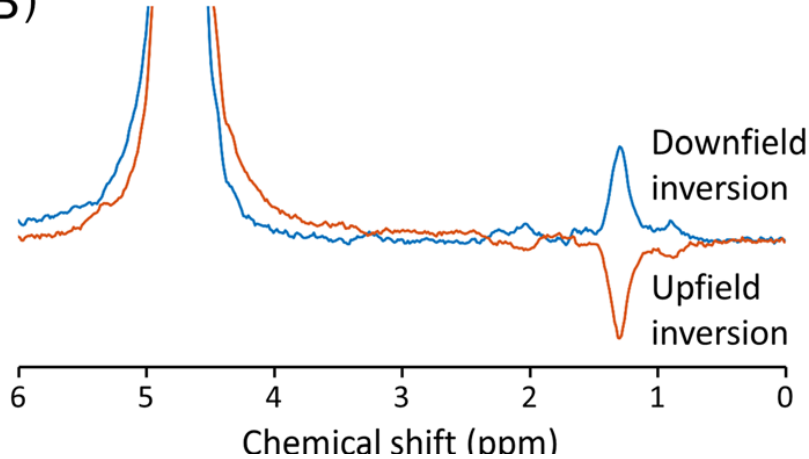
VAPOR



Non-Water Suppression

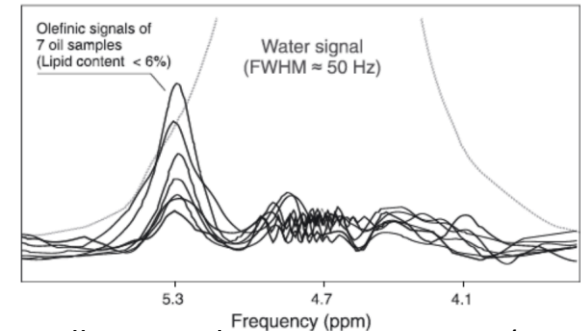


(B)

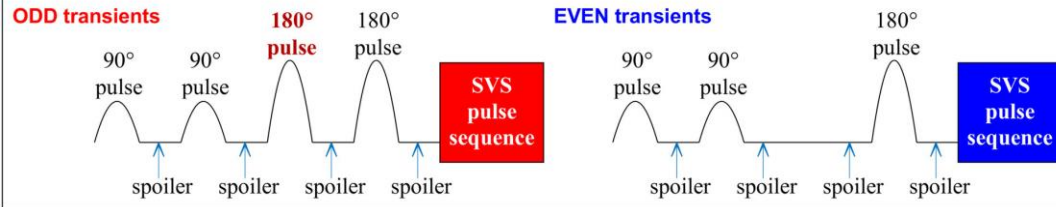


A

Olefinic lipid signals (oil samples)



(A) Water suppression module in pulse sequence



A. Xavier et al., NMR Biomed e4343 (2020)

B. Ding et al., NMR Biomed e4513 (2021)

A. Fillmer et al., Sci Rep 7: 16898 (2017)

M. Gajdošík et al., NMR Biomed e3382 (2015)

Questions?



Artifacts: Signals from Outside the Voxel

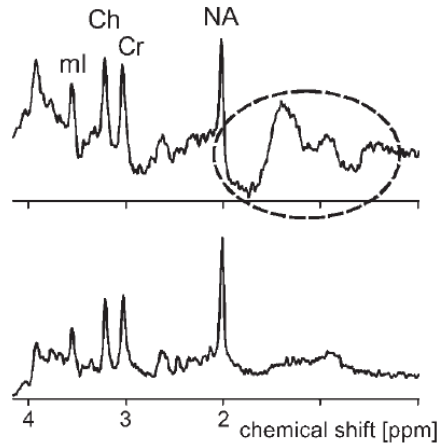


Figure 12. Outer volume lipid contamination. Non-ideal slice selection profiles lead to contamination with outer volume signals. This is particularly relevant if the pulses produce a non-negligible net excitation in areas with lipid deposits that intrinsically give rise to huge signals compared with the metabolite levels. Two fairly old spectra of two male children from a previously published study on brain development, both recorded with a STEAM sequence with identical parameters (TE 30 ms, TR 1.5 s), and similar ROI position (periventricular WM) demonstrate this effect. The top spectrum shows lipid contamination with unclear signal phase, while the lower spectrum demonstrates, what this spectral region normally looks like (adapted from Kreis *et al.*⁴⁰)

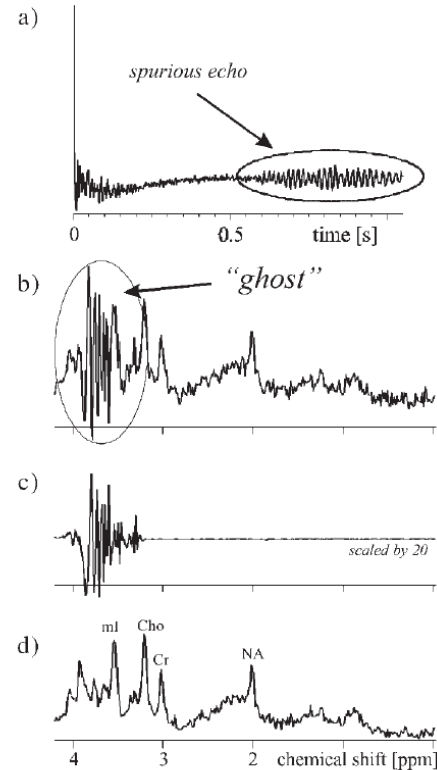


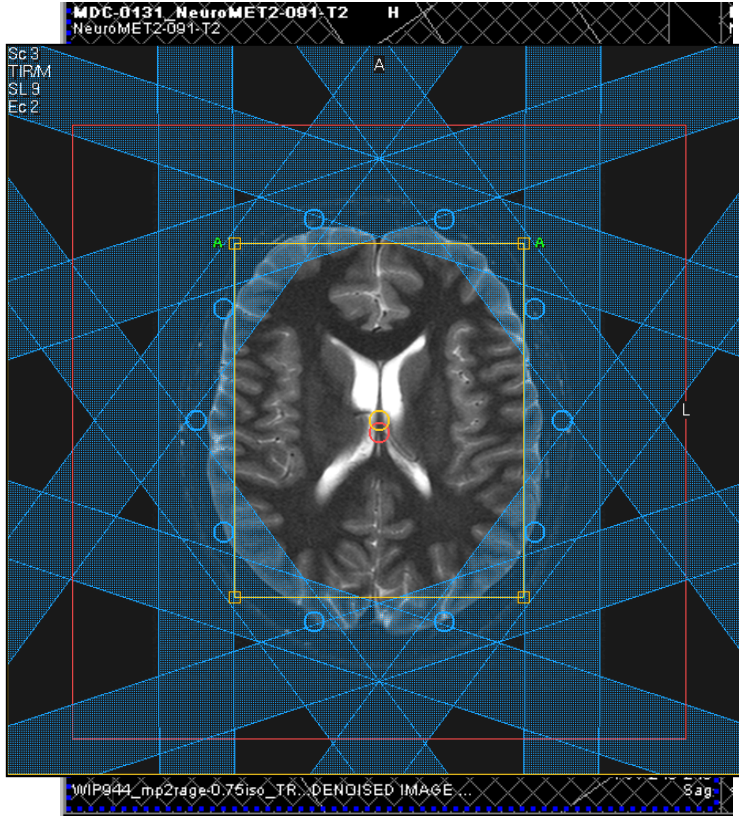
Figure 14. Effect of spurious echoes. Insufficient amplitude of gradient crusher pulses in combination with local B_0 inhomogeneities can lead to the refocusing of unwanted echoes (e.g. 2 pulse echo in a PRESS sequence). (a) The FID from a PRESS acquisition (TE 20 ms, TR 3 s) localizing developing white matter in a female preterm neonate (34 weeks gestational age). The encircled part of the FID originates from an unwanted echo. (b) The typical appearance of spurious echoes, often called ghosts, in the spectrum. Because extended phase cycling was used (phase rotation⁴²) in data acquisition, the origin of the spurious signal could be identified in a separate trace after Fourier transformation along the phase rotation dimension (c). The particular phase evolution proved the spurious signal to arise from a two-pulse echo of the initial 90° and last 180° pulse. In the current case, elimination of the ghosting artifact can easily be accomplished by zeroing the latter half of the FID. The resulting spectrum is plotted in (d)

Artifacts: Signals from Outside the Voxel

Outer Volume Suppression (OVS)



Artifacts: Signals from Outside the Voxel



Outer Volume Suppression (OVS)

Slices placed around the VOI, that are first excited followed by the application of strong gradients

=> signal is dephased and cannot be excited accidentally with the voxel

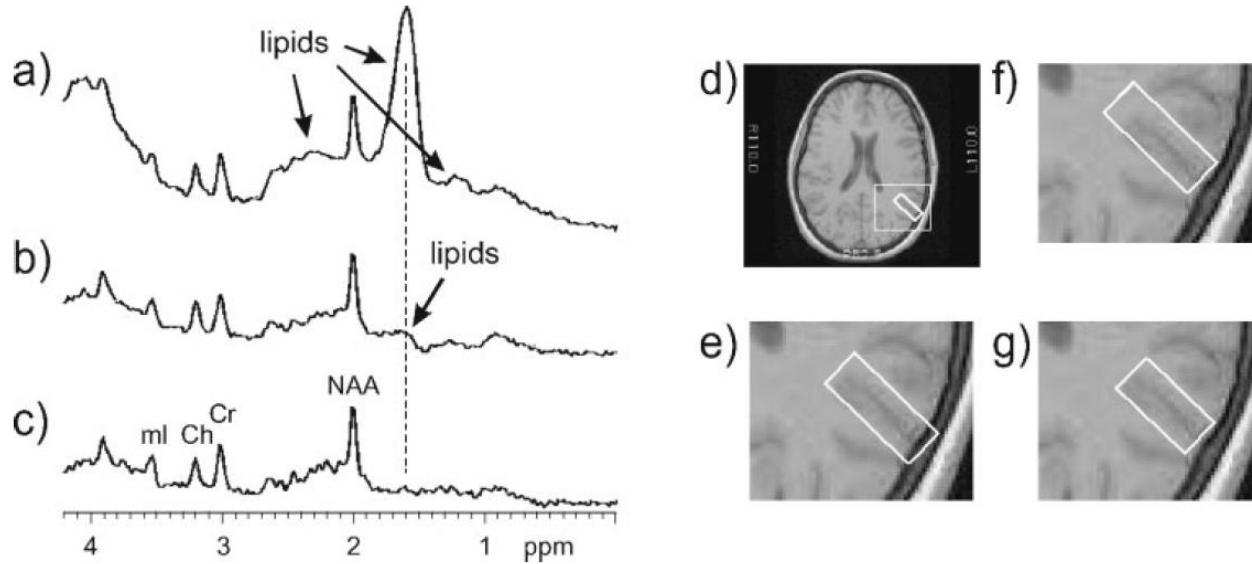


Figure 13. Signal bleed from outside the targeted ROI. Signal from outside the selected ROI can give dominating signal contributions, if the transition zone of the slice selective pulses falls into regions with large lipid content. This is illustrated for PRESS spectra obtained from a 40-year-old woman. The original ROI dimensions of $10 \times 15 \times 27$ mm, used for spectra (a) and (b) were reduced to $10 \times 15 \times 22$ mm for spectrum (c). This diminished the transition zone of the longest dimension of the voxel pointing towards the lipid-containing areas and the lipid contribution vanished. Just moving the ROI away from the skull, (e)–(f), did not completely eliminate the lipid contamination in the spectrum, (a)–(b). (Scan parameters: TE 20 ms, TR 3 s, 1953 Hz spectral width, 1024 points zero-filled to 2048 points, outer volume suppression pulses disabled)

Artifacts: Motion

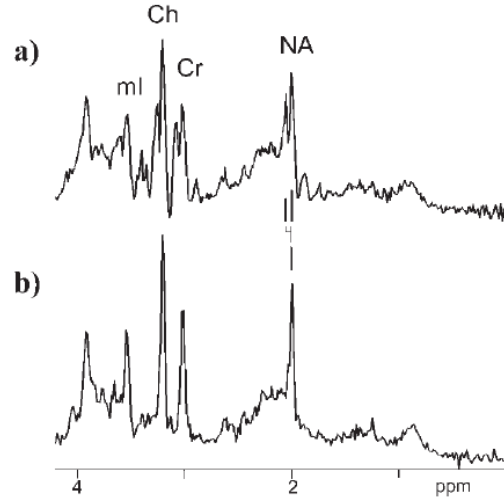
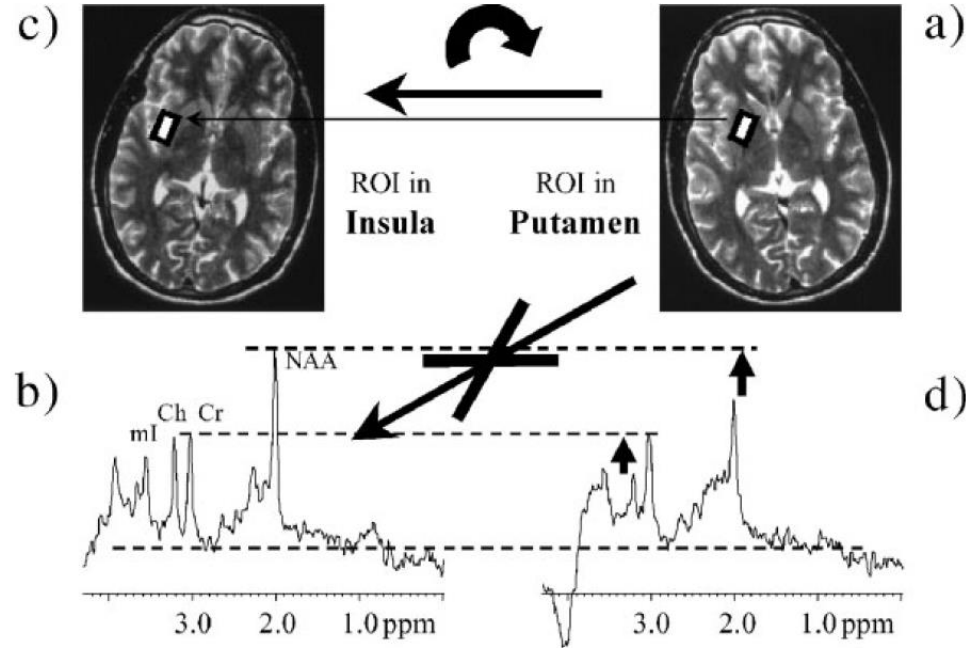
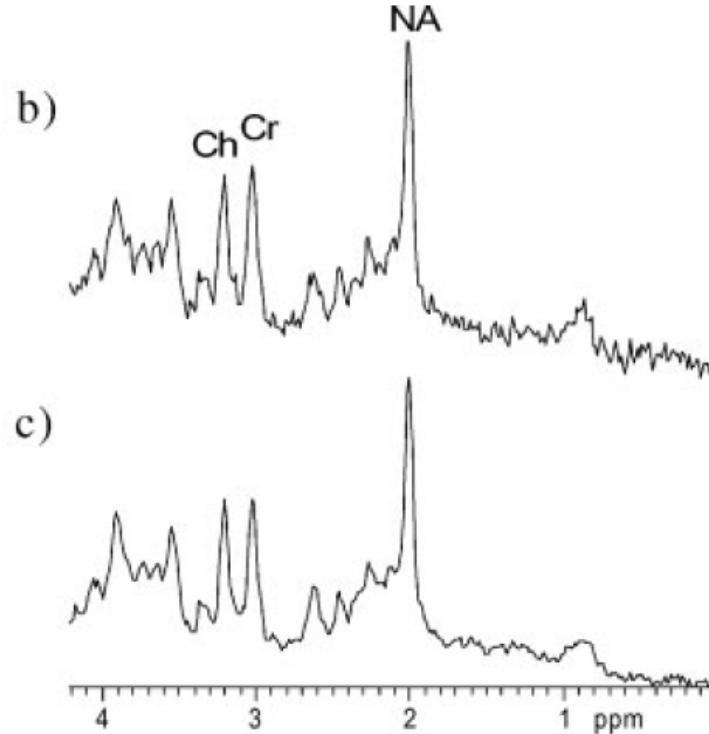
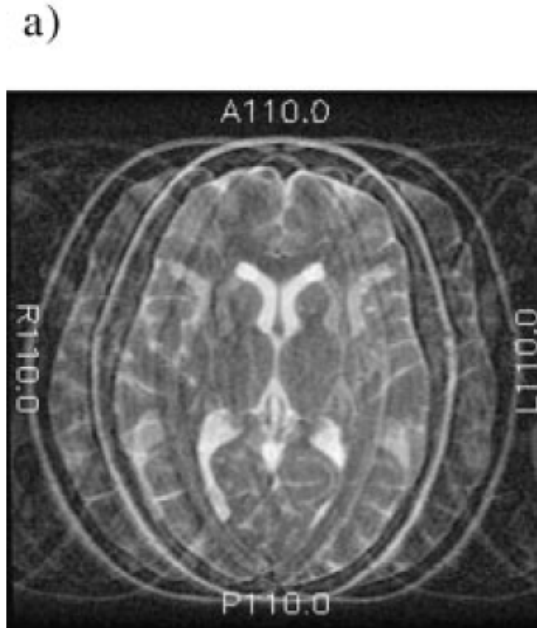


Figure 9. Effect of head movements. All peaks are doubled in a spectrum from a neonate,²¹ because the baby had moved its head between two distinct positions during the scan (a). The repeat examination shows single peaks with perfect shim and lineshape, when the baby was soundly asleep. (Scan parameters: neonate of 41 weeks gestational age, ROI in thalamus, PRESS TE 20 ms, TR 2 s, 128 acquisitions)



R. Kreis, NMR Biomed 17:361-381 (2004)

Artifacts: Motion



Artifacts: Motion



Always export individual transients for optimized postprocessing!

⇒ Cannot compensate for acquiring signal from the wrong region, but

⇒ Can potentially allow correction and, hence, lead to usable spectrum

Questions?



Workflow

